Supporting Information

Stabilizing intermediate phases via efficient confinement effects of SnS_2-SPAN fibre composite for ultra-stable half/full sodium/potassium-ion batteries

Yiyi Wang[a], Xi Chen[a], Xiaochuan Chen[b*], Chuyuan Lin[a], Hong-En Wang[c*], Peixun Xiong[e], Qinghua Chen[a, d], Qingrong Qian[a, d], Mingdeng Wei[e] and Lingxing Zeng[a, d*]

[a] *Engineering Research Centre of Polymer Green Recycling of Ministry of Education, Fujian Key Laboratory of Pollution Control & Resource Reuse, College of Environmental Science and Engineering, Fujian Normal University, Fuzhou, Fujian 350007, China.*

[b] *Key Laboratory for Polymeric Composite and Functional Materials of Ministry of Education, School of Chemistry, Sun Yat-Sen University, Guangzhou, Guangdong, China.*

[c] *College of Physics and Electronics Information, Yunnan Key Laboratory of Optoelectronic Information Technology, Yunnan Normal University, Kunming, 650500, China.*

[d] *Key Laboratory of Advanced Energy Materials Chemistry (Ministry of Education), College of Chemistry, Nankai University, Tianjin 300071, China.*

[e] *Fujian Provincial Key Laboratory of Electrochemical Energy Storage Materials, Fuzhou University, Fuzhou, Fujian 350002, China.*

Experimental

Materials characterization

X-ray diffraction (XRD) test was performed on a Bruker D8 diffractometer to analysis the crystalline structures of samples. The morphologies of samples were investigated by scanning electron microscopy (SEM) and transmission electron microscopy (TEM), using a Hitachi 8100 and FEI F20 S-TWIN equipment, respectively. Raman spectra and FTIR spectroscopy were recorded on a DXR2xi (a diode laser of excitation of 532 nm) and Thermo Scientific Nicolet iS10, respectively. Thermogravimetric analysis (TGA, temperature rises from 30 to 800 ^{o}C in 5 ^{o}C min^{-1}, air) and Electron paramagnetic resonance (EPR) measurement were carried out on a TA-SDT Q600 analyzer and a MS 5000, respectively. X-ray photoelectron spectroscopy (XPS) spectra were applied to study the surface chemical valence states of samples, conducted on an ESCALAB MARK II spherical analyzer.

Electrochemical measurements

The cycle performance of Na/K-ion storage of all the electrodes were investigated by CR2025-type coin cells, which applies pure sodium/potassium metal sheet as the counter/reference electrodes, the glass fiber film (Whatman GF/D) as separator. Active materials, conductive agent (super P) and carboxymethyl cellulose binder (CMC) with a weight ratio of 8:1:1 to fabricate a slurry, then painted on a copper foil followed by dried at 80 ^{o}C in a vacuum overnight to obtain the working electrodes. In which, the mass loading of the active materials on each copper foil was approximately 1-1.5 mg cm^{-2}. The specific capacities of electrodes are calculated based on the total mass of the whole composite. For instance, the capacity of SnS_2-SPAN electrode is calculated based on the total mass of SnS_2 and SPAN. The electrolytes were 1 M $NaPF_6$ in EC/DMC/EMC=1:1:1 with 5% FEC and 7 M KFSI in 100% DME, respectively, for SIBs and PIBs. Additionally, Na-ion full cell was assembled with $Na_3V_2(PO_4)_3$ as cathode and SnS_2-SPAN-470-1 as anode, where the SnS_2-SPAN-470-1 anode was presodiated for several cycles until the CE reached up to 95% before assembling full cells. The capacity ratio of the SnS_2-SPAN-470-1 anode and NVP cathode was optimized to 1: 1.2 in the sodium full-cells. The battery was fabricated in a glove box in an argon atmosphere. The Na/K storage performances and cyclic voltammetry (CV) were tested on a LAND CT 2001A battery tester system with a voltage range of 0.01-3 V and an Ivium-n-Stat electrochemical workstation, respectively.

Computational details

Spin-polarized first-principles density functional theory (DFT) calculations were carried out using projector augmented wave (PAW) pseudopotentials with an exchange-correlation functional of Perdew-Burke-Ernzerhof (PBE) formation implemented in VASP.[S1, S2] An energy cutoff of 400 eV was used for geometry optimization calculations. The simulation box has a size of 20Å×20.1Å×19.9Å for the calculations of adsorption of various species on SPAN or PAN surface. For adsorption calculations on N-doped graphene, a surface slab with a size of 12.8Å×14.8Å×15Å containing 60 C and 9 N atoms were

* Corresponding authors. Tel. & Fax: +86-591 8346 5156.
E-mail addresses: zenglingxing@fjnu.edu.cn (L. Zeng), hongen.wang@outlook.com (H.-E. Wang), chenxch29@mail2.sysu.edu.cn (X. Chen).

adopted. The *k*-point sampling was acquired using a Γ-centered Monkhorst-Pack scheme with a 1×1×1 mesh and 2×2×1 mesh for box containing SPAN (or PAN) and N-doped graphene surface slab, respectively. The convergence criteria for SCF iteration and force were set to 1.0×10^{-5} eV/atom and 0.05 eV/Å, respectively.

The adsorption energies (E_{ads}) were determined using the following equation:

$$E_{ads} = E_{mol/sub} - (E_{mol} + E_{sub})$$

Where $E_{mol/sub}$, E_{mol} and E_{sub} denote the total electronic energies of surface with adsorbed species, and Sn, Na_2S, $SnS_{(2)}$ molecule in gas phase, as well as clean surface, respectively. During the surface calculations, dipole correction was adopted along *z*-axis and van der Waals interactions were considered using DFT-D method. The drawing of the calculated data was performed using VESTA.[S3] Some pre- and post-treatment processes were carried out with the assistance of VASPKIT.[S4]

Supplementary Figures and Tables

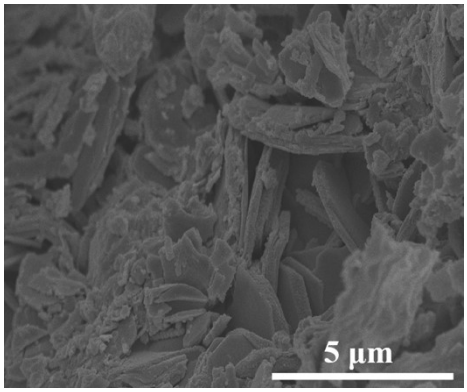

Fig. S1 SEM images of pure SnS_2.

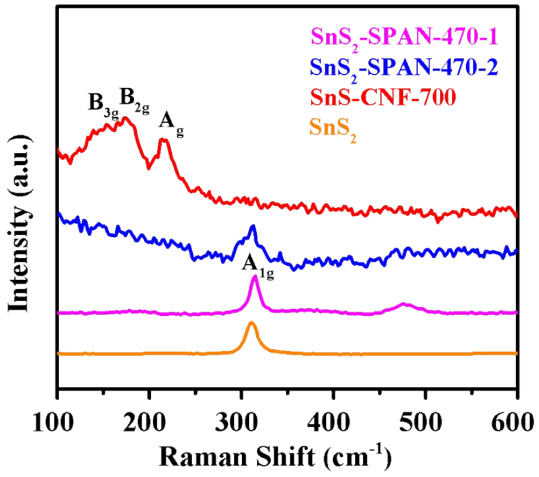

Fig. S2 Raman spectra of the SnS_2-SPAN-470-1, SnS_2-SPAN-470-2, SnS-CNF-700 and pure SnS_2.

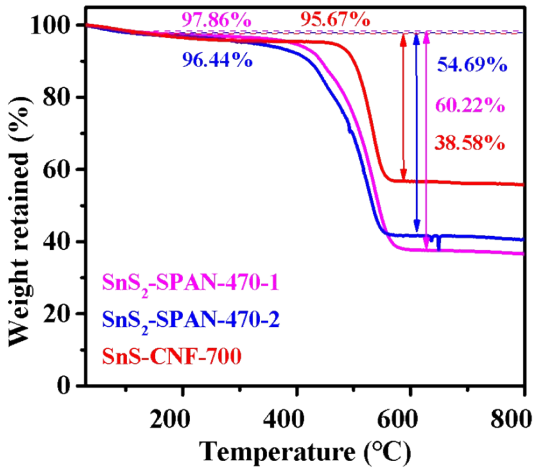

Fig. S3 TG curves of the SnS_2-SPAN-470-1, SnS_2-SPAN-470-2 and SnS-CNF-700 obtained in an air flow at a heating rate of 10 °C min^{-1}.

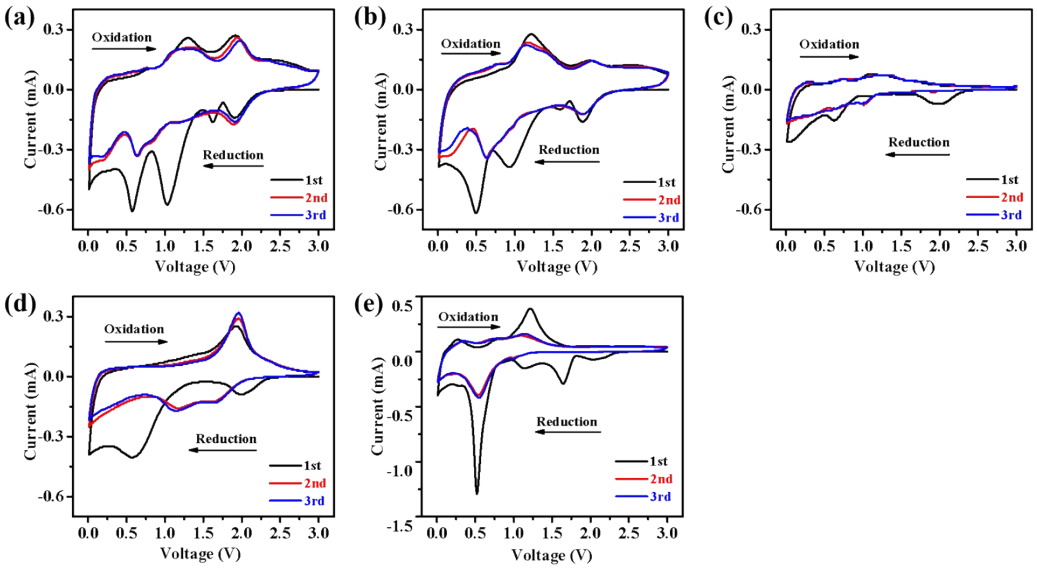

Fig. S4 Cyclic voltammetry curves of (a) SnS_2-SPAN-470-1, (b) SnS_2-SPAN-470-2, (c) SnS-CNF-700, (d) SPAN-470 and (e) pure SnS_2 electrodes at a scan rate of 0.2 mV s^{-1}.

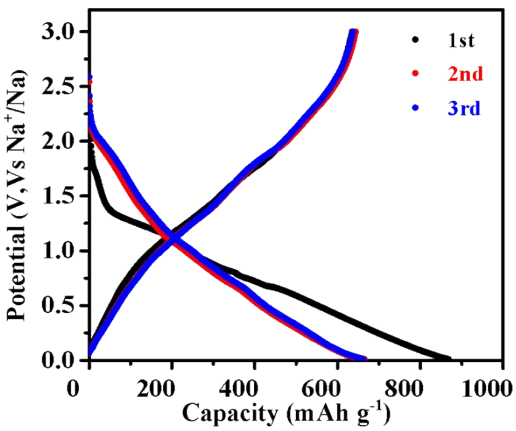

Fig. S5 The charge-discharge profiles of the SnS_2-SPAN-470-1 electrode at 100 mA g^{-1} within a voltage range of 0.01-3.0 V for SIBs.

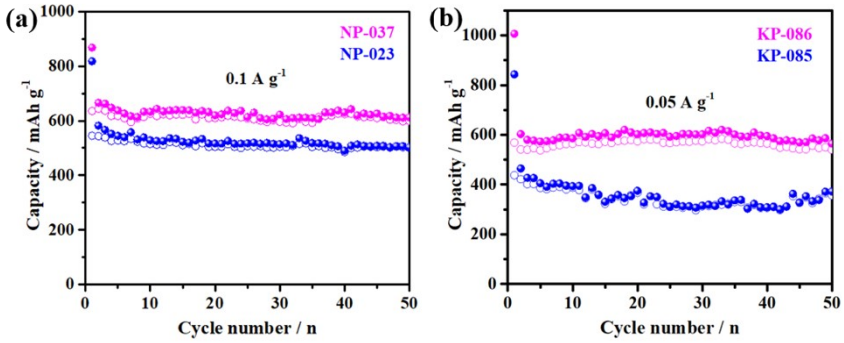

Fig. S6 Cycling performances of SnS_2-SPAN-470-1 electrode in (a) SIBs and (b) PIBs with different electrolytes.

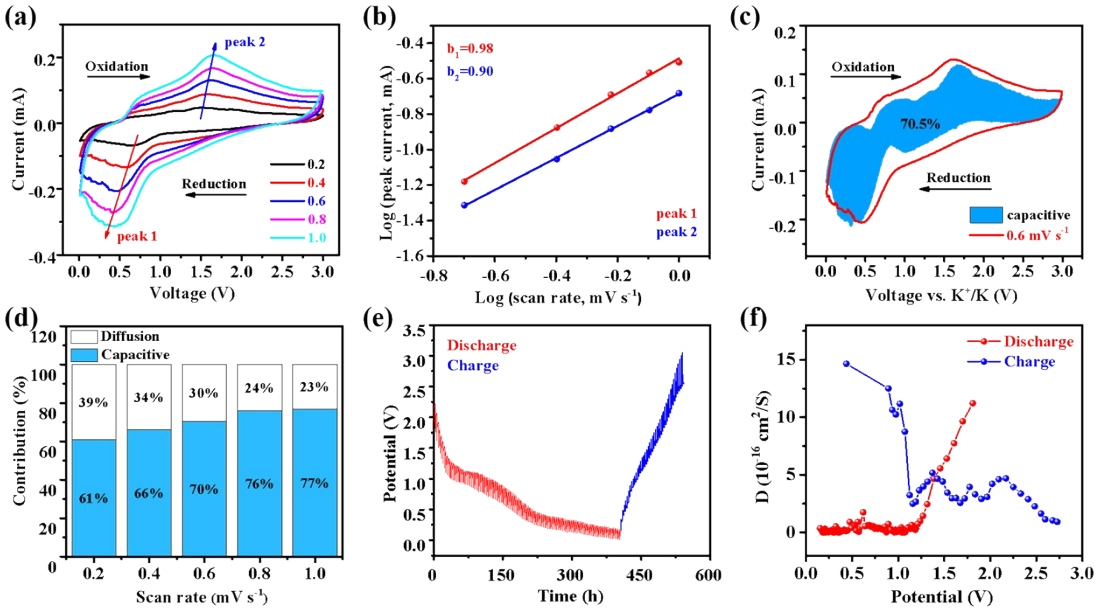

Fig. S7 Electrochemical performances of SnS_2-SPAN-470-1 electrode in PIBs: (a) Cyclic voltammetry curves at various scan rates of 0.2, 0.4, 0.6, 0.8 and 1.0 mV s^{-1}. (b) *b* value determination. (c) Contribution of Capacitive (blue area) at 0.6 mV s^{-1}. (d) Capacitive capacities (blue) and the diffusion controlled (white) at different scan rates. (e) GITT curve. (f) K^+ diffusion coefficients at different voltages.

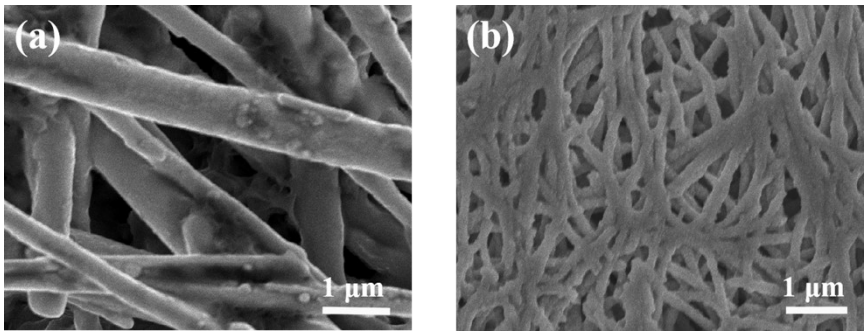

Fig. S8 SEM images of the SnS_2-SPAN-470-1 electrode after 150 cycles at 0.1 A g^{-1} (a) when discharged to 0.02 V for SIBs, (b) when charged to 3.0 V for PIBs.

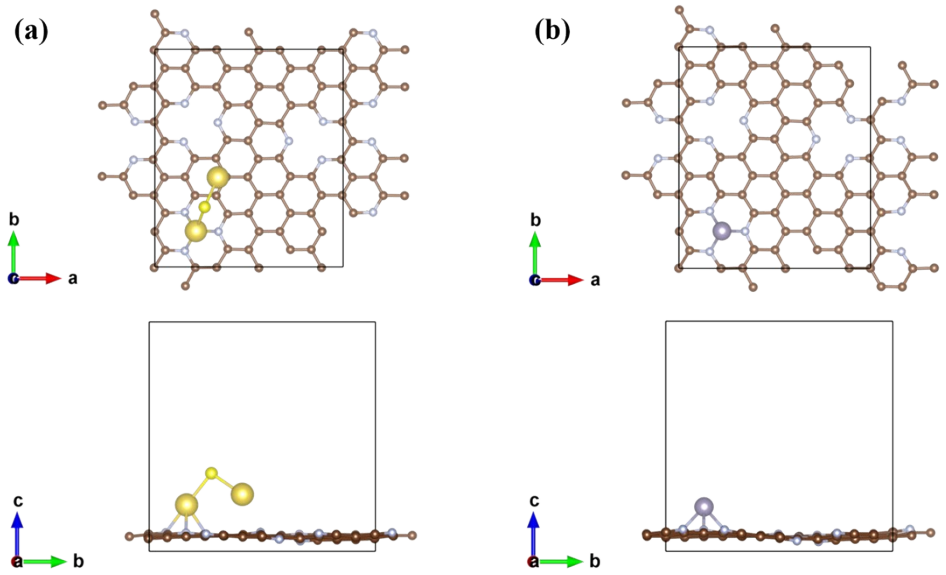

Fig. S9 Adsorption of (a) Na_2S molecule and (b) one Sn atom on N-doped graphene after geometry optimization.

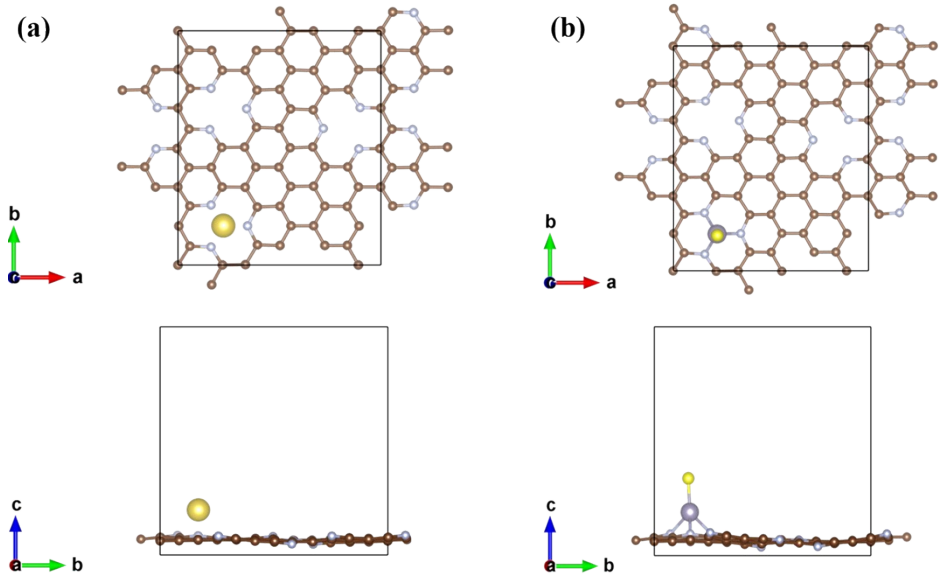

Fig. S10 Adsorption of (a) one Na atom (b) SnS_2 molecule on N-doped graphene after geometry optimization.

Table S1 Electrochemical performance of the SnS_2-SPAN-470-1 and newly reported other anode materials for SIBs/PIBs.

Sample	Fields	Cycling performance			Rate performance		References
		Current density (A g^{-1})	Cycles	Reversible capacity (mAh g^{-1})	Current density (A g^{-1})	Capacity retention (mAh g^{-1})	
SnS_2-SPAN-470-1	SIBs	0.1 5 10	100 10000 30000	613 328 261	30	148	This work
	PIBs	0.05 5	50 2000	565 221	5	172	
PASP@SnS_2@CN	PIBs	0.1 0.5	100 500	372 269	2	273	[32]
GNS@SnS_2/SnS @C	SIBs	0.1	100	476	5	289	[33]
SnS_2@C-1V 1 SMF	PIBs	0.1	100	412	2	138	[41]
N, S-C/SnS_2	PIBs	0.1 2	50 200	503 106	2	105	[40]
SnS_2 NSs/MXene	PIBs	0.05 0.5	100 800	342 206	1	163	[42]
hs-SnS_2	SIBs	0.2 0.5 1	60 100 1000	577 548 486	4	390	[31]
SnS_2@rGO	PIBs	0.05 1	100 300	387 205	0.05 1	442 247	[37]
SnS_2@C-2	PIBs	0.1 2	200 1000	343 183	5	219	[68]
rGO-CoS_2-GNCSs	SIBs	0.1 0.5 1	150 600 400	524 466 412	2	423	[47]
FeS/SPAN-HNF	SIBs	5	500	328	20	126	[45]
NSC	SIBs	0.1 1	100 2000	316 214	3	178	[S5]
TiO_2@$TiOF_2$-30h	SIBs	0.5 5	200 10000	152 101	5	115	[65]
MS-FeSb	SIBs	0.5	80	420	1	300	[66]
MnP_4/G20	SIBs	0.05 0.5	100 250	627 446	2	385	[67]

References

[S1] J. Perdew, K. Burke, M. Ernzerhof, Phys. Rev. Lett., 1996, **77**, 3865-3868.

[S2] G. Kresse, D. Joubert, Phys. Rev. B, 1999, **59**, 1758-1775.

[S3] K. Momma, F. Izumi, J. Appl. Cryst., 2011, **44**, 1272-1276.

[S4] V. Wang, N. Xu, J.-C. Liu, G. Tang, W.-T. Geng, Comp. Phys. Comm., 2021, **267**, 108033.

[S5] J. Li, Z. Ding, L. Pan, J. Li, C. Wang, G. Wang, Carbon, 2021, **173**, 31-40.